

Random walk replicating discrete time quantum walk on one dimension

Tomoki Yamagami ^{1,*}
André Röhm ^{1,3}

Etsuo Segawa ²
Ryoichi Horisaki ¹

Nicolas Chauvet ¹
Makoto Naruse ¹

¹ Department of Information Physics and Computing, Graduate School of Information Science and Technology, The University of Tokyo, 7-3-1 Hongo, Bunkyo, Tokyo 113-8656, Japan.

² Graduate School of Environment and Information Sciences, Yokohama National University, 79-1 Tokiwadai, Hodogaya, Yokohama, Kanagawa 240-8501, Japan.

³ JSPS International Research Fellow.

* Email address: yamagami-tomoki-qwb@g.ecc.u-tokyo.ac.jp [T.Y.]

January 21, 2022

Abstract A quantum walk exhibits quite different properties compared to a classical random walk, such as linear spreading and localization. While quantum superposition provides these interesting properties, their intuitive understanding and characterization are not easy. In this paper, we construct one-dimensional random walks derived by the time evolution of quantum walks and prove that the probability distribution of the original quantum walk and that of the corresponding quantum-walk-replicating random walk is equivalent. Moreover, we demonstrate further insights through the analysis of quantum-walk-replicating random walks, such as the manifestation of linear spreading and localization, by visualizing the traces of individual walkers and transition probabilities.

► We use the following descriptions without notice:

- i is the imaginary unit.
- $\mathbb{N} := \{n \in \mathbb{Z} \mid n \geq 1\}$
- $\mathbb{N}_0 := \{0\} \cup \mathbb{N}$
- For $N \in \mathbb{N}$, $[N] := \{n \in \mathbb{N} \mid 1 \leq n \leq N\}$.
- For $N \in \mathbb{N}$, $[N]_0 := \{n \in \mathbb{N}_0 \mid 0 \leq n \leq N\}$.
- For $a \in \mathbb{R}$, $\text{sgn}(a)$ is the sign of a :

$$\text{sgn}(a) := \begin{cases} -1 & (a < 0) \\ 0 & (a = 0) \\ 1 & (a > 0) \end{cases} .$$

- For $a \in \mathbb{R}$, $\delta_a : \mathbb{R} \rightarrow \{0, 1\}$ is the Dirac's delta:

$$\delta_a(x) = \begin{cases} 1 & (x = a) \\ 0 & (x \neq a) \end{cases} .$$

- For a matrix A , ${}^T A$ and A^* are the transpose and the conjugate transpose of A , respectively.
- The symbols “ $\langle \cdot |$ ” and “ $|\cdot\rangle$ ” are often used as description of row vectors and column vectors, respectively. For a column vector $|x\rangle$, $\langle x| = {}^T |x\rangle$. When we describe inner products with them, we can omit a vertical bar: $\langle x|y\rangle = \langle x|y\rangle$.

1 Introduction

In this paper, we examine the concept of a *quantum-walk-replicating random walk*, which we call QWRW. A quantum walk is often explained as the counterpart of the classical random walk [1–3]. However, the properties of a quantum walk are quite different from the latter. Quantum walks were first introduced in the field of quantum information theory [4, 5]. After that, the characteristic structure of quantum walks was intensively studied by mathematicians, and since then, quantum walks have been an important topic in both fundamental and applied research. Indeed, quantum walks exhibit versatile behavior depending

on conditions or settings of time, space, and thus there are many studies about their mathematical analysis [6–13]. In addition, their unique behavior is useful for implementing quantum structures or quantum analogs of existing models; therefore, the application is considered in the fields such as quantum teleportation [14, 15], time series analysis [16], topological insulators [17, 18], radioactive waste reduction [19, 20], and optics [21].

The particularly unique characteristics of a quantum walk are linear spreading and localization. The former means that the deviation of the distribution of a quantum walk is proportional to its run time. The latter implies that there exist specific positions that have non-zero measurement probability after sufficient time evolution. These interesting properties are, however, not easy to intuitively interpret since they are based on the quantum superposition of multiple states. On the other hand, modified models of classical random walks are widely considered (e.g., correlated random walk [22], Lévy walk [23], Metropolis walk [24]). Such walks are treated as interesting models not only in the field of mathematics but also in natural science [25], economics [26], informatics [27], among others. While the distribution of a simple random walk converges to the normal distribution, those of classical random walks in general do not necessarily do so, including the ones mentioned above. This is why researchers in many fields are interested in them: they can describe more complex transitions of states in real phenomena.

The relationship between quantum walks and modified classical random walks is an active field of study. A related study is given regarding finite graph structures by Andrade et al [28]. In their study, they show the transition probability matrices of quantum walks as non-homogeneous random walks. Our study treats the infinite line (\mathbb{Z}) and examines the associated properties of QWRWs. Our study implies that the discussion on finite graphs is also applied to the part of the infinite graphs. On the study on \mathbb{Z} , the construction of Markov processes is presented by separating the quantum evolution equation into Markovian and interference terms by Romanelli et al [29]. The aim of their decomposition is to show that the linear spreading is derived from coherence. That is, if the equation is decoherent, the spread of the probability distribution goes like simple random walks: the standard deviation is $O(\sqrt{t})$, where t is run time. In the meantime, Montero studied how to obtain the time- and site-dependent coin operator to generate an intended probability distribution on \mathbb{Z} [30]. Therein, the non-homogeneous random walk on \mathbb{Z} exhibiting the identical probability distribution of quantum walk was discussed as a part of interchanging roles.

In this paper, we generate a modified classical random walk by accurately constructing transition probabilities depending on time and position of a quantum walk. We prove that the resulting probability distribution is identical between the QWRW and the original quantum walk. We provide further new insights such as the decision of future directions, transition probabilities of the random walkers replicating quantum walks. Moreover, such a characteristic also gives us new graphical representations on the properties of quantum walks, which are difficult in the conventional theoretical framework of quantum walks. By visualizing the traces of individual walkers and transition probabilities, we will obtain more intuitive understandings of quantum walks and further inspiration of applications. In a sense, one of the primary contributions of the present study is to elaborate the interchanging from quantum walks to random walks examined in [30], and provides further new insights such as the decision of future directions, transition probabilities of the random walkers replicating quantum walks.

The rest of the paper is organized as follows. Section 2 gives the model of one-dimensional simple random walks and quantum walks as preparation. In Sec. 3, we define QWRWs and show that the distribution of QWRWs matches that of quantum walks. Besides, we show examples of QWRWs and visualize their path trajectories and transition probabilities. In Sec. 4, we compare the trajectories of individual walkers for QWRWs and simple classical random walks. Finally, we give a summary and discussion in Sec. 5.

2 Preliminary

In this section, we give the definition of a simple random walk and a two-state quantum walk on \mathbb{Z} .

2.1 Simple random walks

A simple random walk is a stochastic process that describes the motion of a particle on a space. In this paper, we consider discrete simple random walks on \mathbb{Z} . Let S_n be the position of a particle at time $n \in \mathbb{N}_0 = \mathbb{N} \cup \{0\}$. Then the transition of the position is probabilistically determined by the transition probabilities p and q : for a set $(n, x) \in \mathbb{N}_0 \times \mathbb{Z}$,

$$\mathbb{P}(S_{n+1} = x - 1 | S_n = x) = p, \quad \mathbb{P}(S_{n+1} = x + 1 | S_n = x) = q, \quad (1)$$

with $p, q \in [0, 1]$. In this context, p represents the probability that the particle moves at each step one unit to the left side and q represents the probability that the particle moves at each step one unit to the right side. In addition to them, we set $\mathbb{P}(S_{n+1} = y | S_n = x) = 0$ for $y \in \mathbb{Z} \setminus \{x \pm 1\}$. Then by the property of conditional probabilities, p and q are required to satisfy the relationship

$$p + q = 1. \quad (2)$$

Here we define $\nu_n(x)$ as the probability that the particle exists on the position x at time n : for a set $(n, x) \in \mathbb{N}_0 \times \mathbb{Z}$,

$$\nu_n(x) = \mathbb{P}(S_n = x). \quad (3)$$

Then we can derive the following recurrent formula of $\nu_n(x)$:

$$\nu_{n+1}(x) = p\nu_n(x + 1) + q\nu_n(x - 1). \quad (4)$$

Moreover, we put

$$\nu_n = {}^T[\cdots, \nu_n(-1), \nu_n(0), \nu_n(1), \cdots] \quad (5)$$

and

$$M = \begin{bmatrix} \ddots & \vdots & \vdots & \vdots & \vdots & \vdots & \ddots \\ \cdots & 0 & p & 0 & 0 & 0 & \cdots \\ \cdots & q & 0 & p & 0 & 0 & \cdots \\ \cdots & 0 & q & 0 & p & 0 & \cdots \\ \cdots & 0 & 0 & q & 0 & p & \cdots \\ \cdots & 0 & 0 & 0 & q & 0 & \cdots \\ \ddots & \vdots & \vdots & \vdots & \vdots & \vdots & \ddots \end{bmatrix}. \quad (6)$$

We call them the distribution and the transition probability matrix of simple random walks at time n , respectively. Then for $n \in \mathbb{N}_0$, we have

$$\nu_{n+1} = M\nu_n \quad (7)$$

by the recurrent formula of Eq. (4).

2.2 Quantum walks

2.2.1 The definition of quantum walks

First, we give the following unitary matrix:

$$C = \begin{bmatrix} a & b \\ c & d \end{bmatrix}, \quad (8)$$

where $a, b, c, d \in \mathbb{C}$ and $abcd \neq 0$. We call C the coin operator of the quantum walk. Here we consider of the decomposition of C . Let $|L\rangle$ and $|R\rangle$ be ${}^T[1 \ 0]$ and ${}^T[0 \ 1]$, respectively. Using them, we put

$$P = |L\rangle\langle L| C, \quad Q = |R\rangle\langle R| C. \quad (9)$$

Then we obtain

$$C = P + Q, \quad (10)$$

when P and Q give the decomposition of C . P and Q corresponds to the transition probabilities p and q in the context of simple random walks, respectively.

For a set $(n, x) \in \mathbb{N}_0 \times \mathbb{Z}$, we define the vector $\Psi_n(x) \in \mathbb{C}^2$. Here n and x represent the time instant of quantum walks and the position on \mathbb{Z} , respectively. Then $\Psi_n(x)$ stands for the probability amplitude vector of quantum walks on the position x at the time n . We define the time evolution of quantum walks as follow:

$$\Psi_{n+1}(x) = P\Psi_n(x+1) + Q\Psi_n(x-1), \quad (11)$$

which is an analogue of the recurrent formula (4) in the context of simple random walks.

Moreover, for a set (n, x) , we define

$$\mu_n(x) = \|\Psi_n(x)\|^2, \quad (12)$$

where $\mu_n(x)$ now describes the measurement probability of the particle on the position x at the time n .

In the following, we define the system of quantum walks. We put

$$\Psi_n = {}^T[\dots, \Psi_n(-1), \Psi_n(0), \Psi_n(x+1), \dots] \in (\mathbb{C}^2)^{\mathbb{Z}} \quad (13)$$

and

$$U = \begin{bmatrix} \ddots & \vdots & \vdots & \vdots & \vdots & \vdots & \ddots \\ \dots & O & P & O & O & O & \dots \\ \dots & Q & O & P & O & O & \dots \\ \dots & O & Q & O & P & O & \dots \\ \dots & O & O & Q & O & P & \dots \\ \dots & O & O & O & Q & O & \dots \\ \ddots & \vdots & \vdots & \vdots & \vdots & \vdots & \ddots \end{bmatrix}. \quad (14)$$

Then for $n \in \mathbb{N}_0$, we have

$$\Psi_{n+1} = U\Psi_n. \quad (15)$$

Moreover, we define a map $\phi : (\mathbb{C}^2)^{\mathbb{Z}} \rightarrow (\mathbb{R}_{\geq 0})^{\mathbb{Z}}$ with $\mathbb{R}_{\geq 0} = [0, \infty)$ such that

$$\phi(\Psi_n) = {}^T[\dots, \|\Psi_n(-1)\|^2, \|\Psi_n(0)\|^2, \|\Psi_n(1)\|^2, \dots] = {}^T[\dots, \mu_n(-1), \mu_n(0), \mu_n(1), \dots]. \quad (16)$$

Then for any $x \in \mathbb{Z}$, the relationship

$$\phi(\Psi_n)(x) = \phi(\Psi_n(x)) = \|\Psi_n(x)\|^2 = \mu_n(x) \quad (17)$$

holds. In the following, we put $\mu_n = \phi(\Psi_n)$ and call it the distribution of quantum walks at time n .

2.2.2 Examples of quantum walks

Here, we show some examples of quantum walks. Later, we demonstrate QWRWs corresponding to the quantum walks. Most of them have already been well investigated from the perspective of convergence distributions and other properties [6, 7, 11, 12]. In this paper, we treat the corresponding QWRWs of these QWs in the later sections.

Example 1. [Symmetric model]

We set

$$C = \frac{1}{\sqrt{2}} \begin{bmatrix} 1 & 1 \\ 1 & -1 \end{bmatrix}, \quad \Psi_0(x) = \frac{\delta_0(x)}{\sqrt{2}} \begin{bmatrix} 1 \\ i \end{bmatrix}. \quad (18)$$

Then P and Q are calculated as follows:

$$P = |L\rangle\langle L| C = \frac{1}{\sqrt{2}} \begin{bmatrix} 1 & 1 \\ 0 & 0 \end{bmatrix}, \quad Q = |R\rangle\langle R| C = \frac{1}{\sqrt{2}} \begin{bmatrix} 0 & 0 \\ 1 & -1 \end{bmatrix}. \quad (19)$$

Then, the probability amplitudes at time instant $n = 1, 2, 3, 4$ are calculated as follows:

$$\Psi_1(x) = \frac{1}{2} \left(\delta_{-1}(x) \begin{bmatrix} 1+i \\ 0 \end{bmatrix} + \delta_1(x) \begin{bmatrix} 0 \\ 1-i \end{bmatrix} \right), \quad (20)$$

$$\Psi_2(x) = \frac{1}{2\sqrt{2}} \left(\delta_{-2}(x) \begin{bmatrix} 1+i \\ 0 \end{bmatrix} + \delta_0(x) \begin{bmatrix} 1-i \\ 1+i \end{bmatrix} + \delta_2(x) \begin{bmatrix} 0 \\ -1+i \end{bmatrix} \right), \quad (21)$$

$$\Psi_3(x) = \frac{1}{4} \left(\delta_{-3}(x) \begin{bmatrix} 1+i \\ 0 \end{bmatrix} + \delta_{-1}(x) \begin{bmatrix} 2 \\ 1+i \end{bmatrix} + \delta_1(x) \begin{bmatrix} -1+i \\ -2i \end{bmatrix} + \delta_3(x) \begin{bmatrix} 0 \\ 1-i \end{bmatrix} \right), \quad (22)$$

$$\Psi_4(x) = \frac{1}{4\sqrt{2}} \left(\delta_{-4}(x) \begin{bmatrix} 1+i \\ 0 \end{bmatrix} + \delta_{-2}(x) \begin{bmatrix} 3+i \\ 1+i \end{bmatrix} + \delta_0(x) \begin{bmatrix} -1-i \\ 1-i \end{bmatrix} + \delta_2(x) \begin{bmatrix} 1-i \\ -1+3i \end{bmatrix} + \delta_4(x) \begin{bmatrix} 0 \\ -1+i \end{bmatrix} \right). \quad (23)$$

The others are $\mathbf{0}$. Based on them, the probability measures at time instant $n = 1, 2, 3, 4$ are obtained as the following table.

x	-4	-3	-2	-1	0	1	2	3	4
$n = 0$					1				
$n = 1$				1/2		1/2			
$n = 2$			1/4		2/4		1/4		
$n = 3$		1/8		3/8		3/8		1/8	
$n = 4$	1/16		6/16		2/16		6/16		1/16

The probability distribution of this model, shown in Fig. 1(a), exhibits a reverse bell shape, which stems from linear spreading.

Example 2. [Asymmetric model]

We set

$$C = \frac{1}{\sqrt{2}} \begin{bmatrix} 1 & 1 \\ 1 & -1 \end{bmatrix}, \quad \Psi_0(x) = \delta_0(x) \begin{bmatrix} 1 \\ 0 \end{bmatrix}. \quad (24)$$

Then P and Q are calculated as follows:

$$P = |L\rangle\langle L| C = \frac{1}{\sqrt{2}} \begin{bmatrix} 1 & 1 \\ 0 & 0 \end{bmatrix}, \quad Q = |R\rangle\langle R| C = \frac{1}{\sqrt{2}} \begin{bmatrix} 0 & 0 \\ 1 & -1 \end{bmatrix}. \quad (25)$$

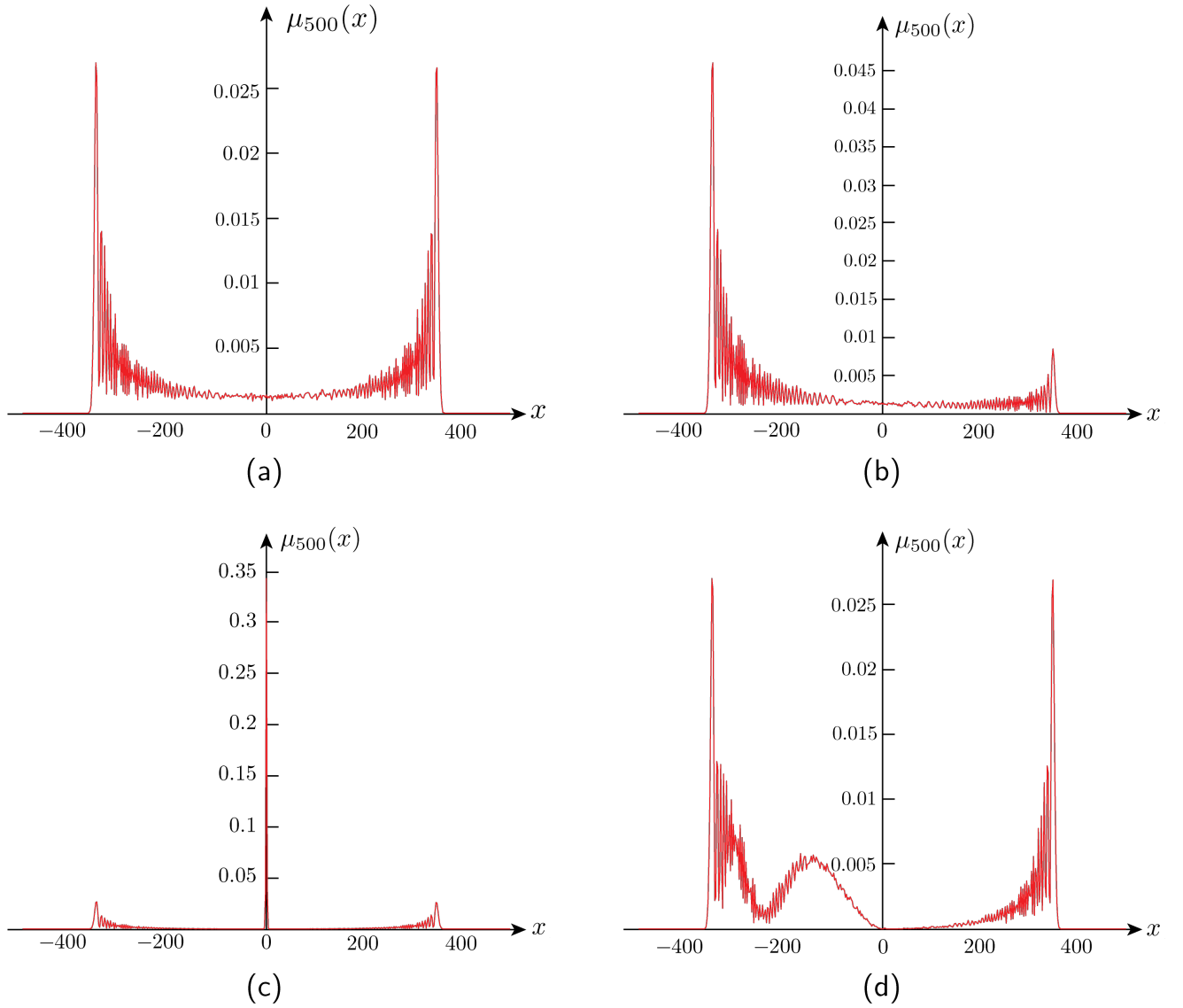


Figure 1: The distributions of QWs (the final time instant $N = 500$, the number of walkers = 100000). (a), (b), (c), and (d) correspond to the Exs. 1, 2, 3, and 4, respectively. Only positions with $\mu_{500}(x) > 0$ are shown. Note the significantly different scaling of the y-axis between subplots.

Then, the probability amplitudes and probabilities are calculated the same as Ex. 1. The probability distribution at time $n = 0, 1, 2, 3, 4$ is obtained as the following table.

x	-4	-3	-2	-1	0	1	2	3	4
$n = 0$					1				
$n = 1$				1/2		1/2			
$n = 2$			1/4		2/4		1/4		
$n = 3$		1/8		5/8		1/8		1/8	
$n = 4$	1/16		10/16		2/16		2/16		1/16

The probability distribution of this model, shown in Fig. 1(b), also exhibits a reverse bell shape, which stems from linear spreading. The distribution is asymmetric, with higher probabilities on the negative side.

The only difference between Exs. 1 and 2 is the initial condition at the origin. The first and second components of the two-dimensional vector correspond to left and right chirality, respectively (The labels L and R in the ket vectors come from “left” and “right”). In Ex. 1, the absolute value of both the first and second component of $\Psi_0(0)$ is $1/\sqrt{2}$, which means that the QWRW tends to go to both sides equally. On the other hand, in Ex. 2, the first component of $\Psi_0(0)$ is 1, and the second is 0, which means that the QWRW tends to go to the left side. This illustrates, how the properties of a quantum walk are sensitive to the initial state even for identical coin operators.

Example 3. [One-defect at the center model]

In this example, the coin operator depends on the position of walkers:

$$C = C_x = \begin{cases} \begin{bmatrix} 1 & 0 \\ 0 & 1 \end{bmatrix} & (x = 0) \\ \frac{1}{\sqrt{2}} \begin{bmatrix} 1 & 1 \\ 1 & -1 \end{bmatrix} & (\text{otherwise}) \end{cases}, \quad (26)$$

$$\Psi_0(x) = \frac{\delta_0(x)}{\sqrt{2}} \begin{bmatrix} 1 \\ i \end{bmatrix}. \quad (27)$$

Then the probability amplitudes and probabilities are calculated the same as Ex. 1. The probability distribution at time $n = 0, 1, 2, 3, 4$ is obtained as the following table.

x	-4	-3	-2	-1	0	1	2	3	4
$n = 0$					1				
$n = 1$				1/2		1/2			
$n = 2$			1/4		2/4		1/4		
$n = 3$		1/8		3/8		3/8		1/8	
$n = 4$	1/16		4/16		6/16		4/16		1/16

This setting is called the one-defect at the center model. As we can observe in Fig. 1(c), the QWRW derived from this model exhibits localization at $x = 0$ as well as linear spreading.

Example 4. [One-defect near the center model]

In this example, the coin operator depends on the position of walkers:

$$C = C_x = \begin{cases} \begin{bmatrix} 1 & 0 \\ 0 & 1 \end{bmatrix} & (x = 5) \\ \frac{1}{\sqrt{2}} \begin{bmatrix} 1 & 1 \\ 1 & -1 \end{bmatrix} & (\text{otherwise}) \end{cases}, \quad (28)$$

$$\Psi_0(x) = \frac{\delta_0(x)}{\sqrt{2}} \begin{bmatrix} 1 \\ i \end{bmatrix}. \quad (29)$$

The difference with Ex. 3. is the position of the defect coin. When the position of the defect coin doesn't match that of the initial state, the distribution does not have the peak on the origin. Instead Fig. 1(d) shows low probabilities around the defect site, and higher probabilities on the opposite of the origin.

3 Quantum-walk-replicating random walk

In this section, we present the quantum-walk-replicating random walk (QWRW). First, we describe the way of constructing the QWRW. In this study, we limit the target to \mathbb{Z} . We then show that the

probability distribution of a QWRW matches that of the corresponding quantum walk by giving an initial condition for both of them. Second, some examples of QWRWs are provided, and we examine the properties of QWRWs through these examples.

3.1 The construction of QWRWs

In this subsection, we construct QWRWs. For a set $(n, x) \in \mathbb{N}_0 \times \mathbb{Z}$ such that $\mu_n(x) > 0$, the transition probabilities of the random walks are defined by the following quantity:

$$p_n(x) = \frac{\|P\Psi_n(x)\|^2}{\mu_n(x)}, \quad q_n(x) = \frac{\|Q\Psi_n(x)\|^2}{\mu_n(x)}. \quad (30)$$

Here for $p_n(x)$ and $q_n(x)$, the following Propositions 1 and 2 hold, which are important to construct the distribution.

Proposition 1. *For a set $(n, x) \in \mathbb{N}_0 \times \mathbb{Z}$ such that $\mu_n(x) > 0$,*

$$0 \leq p_n(x) \leq 1 \quad \text{and} \quad 0 \leq q_n(x) \leq 1. \quad (31)$$

Proof. Here we show this proposition for $p_n(x)$. We can obtain the conclusion for $q_n(x)$ by making a similar discussion.

By the property of norms and the assumption $\mu_n(x) > 0$, the inequality

$$0 \leq p_n(x) \quad (32)$$

is trivial. We define $\langle P_L | = [a, b]$, which leads to $\|P\Psi_n(x)\|^2 = |\langle P_L | \Psi_n(x) \rangle|^2$. By Cauchy-Schwarz inequality,

$$|\langle P_L | \Psi_n(x) \rangle|^2 \leq \|P_L\|^2 \cdot \|\Psi_n(x)\|^2 = (|a|^2 + |b|^2)\mu_n(x). \quad (33)$$

Here the relationship $\|P_L\|^2 = |a|^2 + |b|^2 = 1$ holds by the unitarity of the coin operator C . Therefore we obtain the inequality

$$\|P\Psi_n(x)\|^2 \leq \mu_n(x) \iff p_n(x) = \frac{\|P\Psi_n(x)\|^2}{\mu_n(x)} \leq 1. \quad (34)$$

Combining (32) and (34), we obtain the desired result. \square

Proposition 2. *For a set $(n, x) \in \mathbb{N}_0 \times \mathbb{Z}$ such that $\mu_n(x) > 0$,*

$$p_n(x) + q_n(x) = 1. \quad (35)$$

Proof. By unitarity of the coin operator C and the Eq. (10), we obtain

$$\mu_n(x) = \|\Psi_n(x)\|^2 = \|C\Psi_n(x)\|^2 = \|P\Psi_n(x) + Q\Psi_n(x)\|^2. \quad (36)$$

Here the relational expression $\langle L|R \rangle = \langle R|L \rangle = 0$ holds, which leads to

$$\|P\Psi_n(x) + Q\Psi_n(x)\|^2 \quad (37)$$

$$= \left(\langle \Psi_n(x) | C^* | L \rangle \langle L | + \langle \Psi_n(x) | C^* | R \rangle \langle R | \right) \left(| L \rangle \langle L | C | \Psi_n(x) \rangle + | R \rangle \langle R | C | \Psi_n(x) \rangle \right) \quad (38)$$

$$= \|P\Psi_n(x)\|^2 + \|Q\Psi_n(x)\|^2. \quad (39)$$

Therefore,

$$\|P\Psi_n(x)\|^2 + \|Q\Psi_n(x)\|^2 = \mu_n(x) \iff p_n(x) + q_n(x) = 1. \quad (40)$$

This is the desired equation. \square

By the propositions above, we can define QWRW as follows:

Definition 3. [quantum-walk-replicating random walk (QWRW)]

Let $\{\Psi_n\}_{n \in \mathbb{N}_0}$ be the quantum walk defined by (15), i.e.,

$$\Psi_{n+1} = P\Psi_n(x+1) + Q\Psi_n(x-1), \quad \Psi_0(x) = \delta_0(x)\varphi_0 \quad (41)$$

with $\|\varphi_0\| = 1$. The quantum-walk-replicated random walk (QWRW) $\{S_n\}_{n \in \mathbb{N}_0}$ satisfies the following evolution: for $(n, x) \in \mathbb{N}_0 \times \mathbb{Z}$ such that $\mu_n(x) > 0$,

$$\mathbb{P}(S_{n+1} = x + \xi \mid S_n = x) = \begin{cases} p_n(x) & : \xi = -1 \\ q_n(x) & : \xi = +1 \\ 0 & : \text{otherwise} \end{cases}, \quad (42)$$

where $p_n(x) = \frac{\|P\Psi_n(x)\|^2}{\mu_n(x)}$ and $q_n(x) = \frac{\|Q\Psi_n(x)\|^2}{\mu_n(x)}$.

Let $\tilde{\nu}_n(x)$ be the probability that a particle following QWRW (a QWRWer) exists on $x \in \mathbb{Z}$ at the time $n \in \mathbb{N}_0$. In other words, $\tilde{\nu}_n(x)$ is defined by the initial distribution and the following recurrent formula:

$$\tilde{\nu}_{n+1}(x) = p_n(x+1)\tilde{\nu}_n(x+1) + q_n(x-1)\tilde{\nu}_n(x-1). \quad (43)$$

Moreover, we put

$$\tilde{\nu}_n = {}^T[\cdots, \tilde{\nu}_n(-1), \tilde{\nu}_n(0), \tilde{\nu}_n(1), \cdots] \quad (44)$$

and call it the distribution of QWRWs at time n .

Incidentally, we have the following lemma:

Lemma 4. For $n \in \mathbb{N}_0$,

$$\mu_{n+1}(x) = p_n(x+1)\mu_n(x+1) + q_n(x-1)\mu_n(x-1). \quad (45)$$

Proof. By Eq. (11),

$$\begin{aligned} \mu_{n+1}(x) &= \|\Psi_{n+1}(x)\|^2 = \|P\Psi_n(x+1) + Q\Psi_n(x-1)\|^2 \\ &= \left(\langle \Psi_n(x+1) | C^* | L \rangle \langle L | + \langle \Psi_n(x-1) | C^* | R \rangle \langle R | \right) \left(|L\rangle \langle L| C | \Psi_n(x+1)\rangle + |R\rangle \langle R| C | \Psi_n(x-1)\rangle \right) \\ &= \|\langle L | C | \Psi_n(x+1)\rangle\|^2 + \|\langle R | C | \Psi_n(x-1)\rangle\|^2 = \|P\Psi_n(x+1)\|^2 + \|Q\Psi_n(x-1)\|^2. \end{aligned} \quad (46)$$

By the definition of $p_n(x)$ and $q_n(x)$ (30), we obtain the desired conclusion. \square

Using Lemma 4, we obtain the following fact: if and only if we assume $\tilde{\nu}_0 = \mu_0$, the distribution of QWRWs and QWs coincident completely. Therefore, we can draw the following theorem:

Theorem 5.

$$\tilde{\nu}_0 = \mu_0 \iff \tilde{\nu}_n = \mu_n \text{ for all } n \in \mathbb{N}_0. \quad (47)$$

Proof. We assume that for time instant $n \in \mathbb{N}_0$

$$\tilde{\nu}_n = \mu_n. \quad (48)$$

Then using the relational expression (43) and the assumption above, we have

$$\tilde{\nu}_{n+1}(x) = p_n(x+1)\mu_n(x+1) + q_n(x-1)\mu_n(x-1) \quad (49)$$

for any $x \in \mathbb{Z}$. Therefore, by the Lemma 4, we obtain

$$\tilde{\nu}_{n+1}(x) = \mu_{n+1}(x). \quad (50)$$

Reminding that this holds for any $x \in \mathbb{Z}$, we obtain the desired conclusion. \square

Here we compare our theory with previous studies. Ours extends Theorem 1 in [28] to an infinite graph if we consider numbers of position $x \in \mathbb{Z}$ as labels of vertices on the infinite graph $G(\mathbb{Z}, E_{\mathbb{Z}})$ with $E_{\mathbb{Z}} = \{(x, y) \in \mathbb{Z}^2 \mid |x - y| = 1\}$. Our definition of transition probabilities (30) corresponds to the case that $v(u, t) > 0$ and $(u, v) \in E$ in Eq. (18) in their results, which is the case that $\mu_n(x) > 0$ and $(x, y) \in E_{\mathbb{Z}}$ in our contexts. Note that $\rho(v, c, t + 1)$ in their paper corresponds to the left (resp. right) chirality of $\Psi_{n+1}(x - 1)$ ($\Psi_{n+1}(x + 1)$), whose value matches the left (right) component of $P\Psi_n(x)$ ($Q\Psi_n(x)$). The difference of our study from their result is that the identification between the distribution of quantum walk (μ_n) and QWRW ($\tilde{\nu}_n$) is the theorem as we showed in Theorem 5 while they assume the match between quantum walk ($v(v, t)$) and non-homogeneous random walk ($\pi_v(t)$).

In [30], almost the same model is generated as a result of interchanging roles, which solve the problem of how a time- and site-dependent random walk mimics the properties of a quantum walk or the opposite situation. There time- and site-dependent random walk and quantum walk are combined by equating both of the net fluxes, which are

$$J_n^{(\text{RW})}(x) = (q_n(x) - p_n(x))\tilde{\nu}_n(x) \quad \text{and} \quad J_n^{(\text{QW})}(x) = \|Q\Psi_n(x)\|^2 - \|P\Psi_n(x)\|^2 \quad (51)$$

respectively, in our contexts. However, this theory also needs the assumption that the distribution of time- and site-dependent random walk and that of quantum walk are the same, which are described as $\rho(n, t)$ in [30]. In this sense, our introduction of the distribution is made in the opposite direction to their paper.

3.2 Symmetric example using QWRW

In this subsection, we present an example of generating a QWRW from a QW. We can illustrate how the probability distributions of a QWRW is identical to that of the corresponding quantum walk.

Here, we demonstrate an example of a QWRW for Ex. 1. We set

$$C = \frac{1}{\sqrt{2}} \begin{bmatrix} 1 & 1 \\ 1 & -1 \end{bmatrix}, \quad \Psi_0(x) = \frac{\delta_0(x)}{\sqrt{2}} \begin{bmatrix} 1 \\ i \end{bmatrix}. \quad (52)$$

Then P and Q are calculated as follows:

$$P = |L\rangle\langle L| C = \frac{1}{\sqrt{2}} \begin{bmatrix} 1 & 1 \\ 0 & 0 \end{bmatrix}, \quad Q = |R\rangle\langle R| C = \frac{1}{\sqrt{2}} \begin{bmatrix} 0 & 0 \\ 1 & -1 \end{bmatrix}. \quad (53)$$

As in Ex. 1 of the quantum walks, the probability at time $n = 0$ is defined as follows:

$$\tilde{\nu}_0(0) = \mu_0(0) = 1. \quad (54)$$

The probabilities $p_0(0)$ and $q_0(0)$ are calculated as follows:

$$p_0(0) = \frac{\|P\Psi_0(0)\|^2}{\mu_0(0)} = \left\| \frac{1}{2} \begin{bmatrix} 1+i \\ 0 \end{bmatrix} \right\|^2 = \frac{1}{2}, \quad q_0(0) = \frac{\|Q\Psi_0(0)\|^2}{\mu_0(0)} = \left\| \frac{1}{2} \begin{bmatrix} 0 \\ 1-i \end{bmatrix} \right\|^2 = \frac{1}{2}. \quad (55)$$

Therefore, the existence probabilities at time $n = 1$ are obtained as follows:

$$\tilde{\nu}_1(-1) = p_0(0)\tilde{\nu}_0(0) = \frac{1}{2}, \quad \tilde{\nu}_1(1) = q_0(0)\tilde{\nu}_0(0) = \frac{1}{2} \quad (56)$$

The probabilities $p_1(\pm 1)$, $q_1(\pm 1)$ are calculated as follows:

$$p_1(-1) = \frac{\|P\Psi_1(-1)\|^2}{\mu_1(-1)} = 2 \left\| \frac{1}{2\sqrt{2}} \begin{bmatrix} 1+i \\ 0 \end{bmatrix} \right\|^2 = \frac{1}{2}, \quad q_1(-1) = \frac{\|Q\Psi_1(-1)\|^2}{\mu_1(-1)} = 2 \left\| \frac{1}{2\sqrt{2}} \begin{bmatrix} 0 \\ 1+i \end{bmatrix} \right\|^2 = \frac{1}{2}, \quad (57)$$

$$p_1(1) = \frac{\|P\Psi_1(1)\|^2}{\mu_1(1)} = 2 \left\| \frac{1}{2\sqrt{2}} \begin{bmatrix} 1-i \\ 0 \end{bmatrix} \right\|^2 = \frac{1}{2}, \quad q_1(1) = \frac{\|Q\Psi_1(1)\|^2}{\mu_1(1)} = 2 \left\| \frac{1}{2\sqrt{2}} \begin{bmatrix} 0 \\ -1+i \end{bmatrix} \right\|^2 = \frac{1}{2}. \quad (58)$$

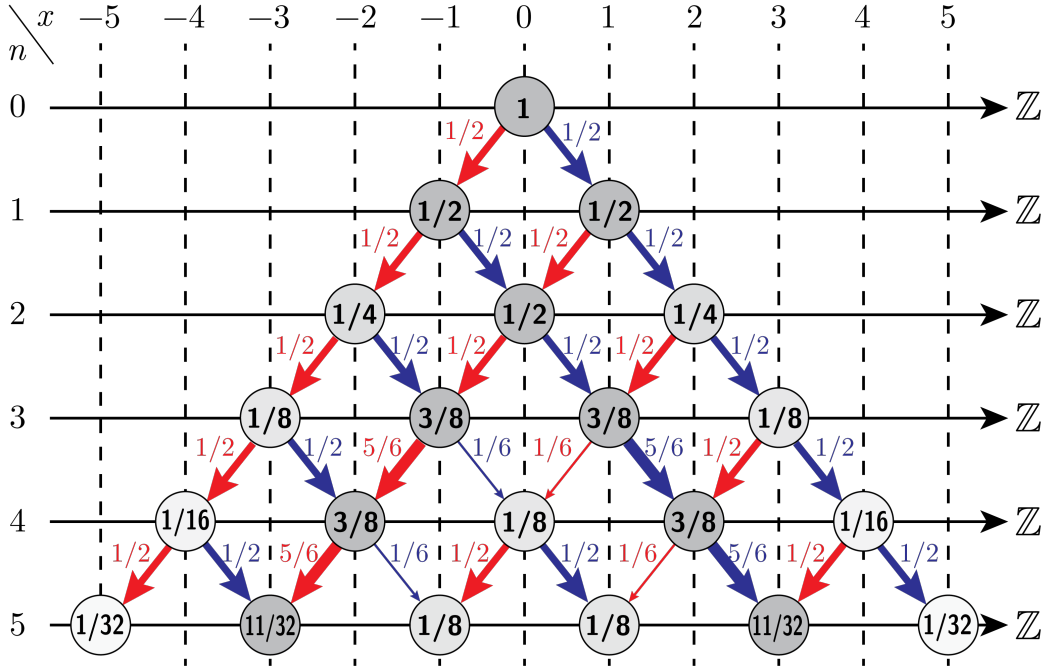


Figure 2: Transition of the distribution $\tilde{\nu}_n$ of the QWRW corresponding to the symmetric case of Ex. 1. Red and blue arrows represent $p_n(x)$ and $q_n(x)$ from each set (n, x) , respectively. Values on each coordinate (n, x) represents the corresponding value of $\tilde{\nu}(x)$. For the coordinates that don't have any display about $\tilde{\nu}_n(x)$, their values are 0.

Therefore, the existence probabilities at time $n = 2$ are obtained as follows:

$$\tilde{\nu}_2(-2) = p_1(-1)\tilde{\nu}_1(-1) = \frac{1}{4}, \quad \tilde{\nu}_2(0) = p_1(1)\tilde{\nu}_1(1) + q_1(-1)\tilde{\nu}_1(-1) = \frac{1}{2}, \quad \tilde{\nu}_2(2) = q_1(1)\tilde{\nu}_1(1) = \frac{1}{4}. \quad (59)$$

The probabilities $p_2(0)$, $q_2(0)$, $p_2(\pm 2)$, $q_2(\pm 2)$ are calculated as follows:

$$p_2(0) = q_2(0) = p_2(2) = q_2(2) = p_2(-2) = q_2(-2) = \frac{1}{2}. \quad (60)$$

Therefore, the existence probabilities at time $n = 3$ are obtained as follows:

$$\tilde{\nu}_3(-3) = \tilde{\nu}_3(3) = \frac{1}{8}, \quad \tilde{\nu}_3(-1) = \tilde{\nu}_3(1) = \frac{3}{8}. \quad (61)$$

Until then, the probabilities are the same as the simple random walk, but this shall not apply to further behavior. The transition probabilities at $n = 3$ are calculated as follows:

$$p_3(-3) = q_3(-3) = p_3(3) = q_3(3) = \frac{1}{2}, \quad (62)$$

$$p_3(-1) = q_3(1) = \frac{5}{6}, \quad q_3(-1) = p_3(1) = \frac{1}{6}. \quad (63)$$

Therefore, the existence probabilities at time $n = 4$ are obtained as follows:

$$\tilde{\nu}_4(-4) = \tilde{\nu}_4(4) = \frac{1}{16}, \quad \tilde{\nu}_4(-2) = \tilde{\nu}_4(2) = \frac{3}{8}, \quad \tilde{\nu}_4(0) = \frac{1}{8}. \quad (64)$$

Similarly, transition and existence probabilities are calculated like Fig. 2. From these results, we can check that the distribution of QWRW ($\tilde{\nu}_n(x)$) and that of QW ($\mu_n(x)$ in Ex. 1 of QW) match.

3.3 Graphical representations of the transition probabilities

In this subsection, we show graphical representations for the QWRWs corresponding to examples 1, 2, 3, and 4. While the existence probabilities $\tilde{\nu}_n$ reproduce those of previously studied QWs, the transition probabilities p_n and q_n can now be visualized with the help of QWRWs and reveal an intricate pattern.

3.3.1 Probability distributions

Figure 3 shows two types of representations regarding the probability distributions $\tilde{\nu}_n(x)$ for the different examples of QWRWs. The upper figure of each panel shows the space-time diagrams of the early evolution of the probability distributions from $n = 0$ to $n = 15$. Here, time progresses downwards and the darker color indicates a large value of $\tilde{\nu}_n(x)$. We can clearly observe different space-time evolution of the probabilities depending on the four models. In Ex. 1 (Fig. 3(a)), the dark color circular marks are observed at the left and the right side, showing the linear spreading typically associated with QWs. Conversely, in Ex. 2 (Fig. 3(b)), the darker markers are observed only on the left side, manifesting the asymmetric linear spreading. For the single-defect at the origin explored in Ex. 3 (Fig. 3(c)), the larger probability positions are observed around the origin. Meanwhile, slightly larger-valued probabilities are observed at the left and right sides. That is, the properties of linear spreading and localization are clearly indicated. Finally, in Ex. 4 (Fig. 3(d)), the influence of the defect coin at $x = 5$ can be clearly seen, destroying the symmetry.

The lower figure of each panel shows the probability distributions of QWRWs for the time instant $n = 500$, which exactly matches with the probability distribution obtained via the original QW (Fig. 1). As discussed above, QWRWs inherit the properties of QWs. Also, these graphical illustrations help intuitive understandings of Theorem 3.

3.3.2 Transition probabilities

Second, we examine the expressions of transition probabilities $p_n(x)$ and $q_n(x)$. The sum of $p_n(x)$ and $q_n(x)$ is equal to 1; hence our interest is in the imbalances between $p_n(x)$ and $q_n(x)$. The blue and red portion of the color bars in Fig. 4 indicates the amount of $p_n(x)$ and $q_n(x)$, respectively. A common attribute observed in Figs. 4(a), (b), (c), and (d) is that there are peaks of $p_n(x)$ and $q_n(x)$ on the left and right sides, respectively. For $x \leq -350$ and $x \geq 350$ all examples have identical transition probabilities, following a simple quasi-continuous function of x . This part of the transition probabilities indicates that individual walkers that go far away from the origin tend to go farther, which is related to the linear spreading property of QWs.

In the centre region of Fig. 4, the transition probabilities are fluctuating quickly as a function of x . These fluctuations are quasi-continuous around the origin, but become discontinuous for $x \rightarrow \pm 350$. The exact position and height of these maxima and minima in $p_n(x)$ and $q_n(x)$ also changes with n .

A big differences among the different examples shown in Fig. 4 is the distribution around the origin. In Fig. 4(a), $p_n(x)$ exhibits a peak on the left side of the origin while $q_n(x)$ shows a peak on the right side of the origin. This means that the QWRWs starting from the origin equally likely go to the left side or to the right side. This is strongly related to the fact that the probability distribution $\tilde{\nu}_n(x)$ in Ex. 1 exhibits its highest peaks on both left and right sides (Fig. 3(a)). Conversely, in Fig. 4(b), $p_n(x)$ exhibits its local maximum at both sides of the origin. This means that QWRWs are highly likely to move toward the left side, which agrees with the asymmetric probability distribution in Fig. 3(b). In Fig. 4(c), on the other hand, $p_n(x)$ and $q_n(x)$ show the local maximum on the right and left sides, respectively, meaning that the QWRWs are guided toward opposite directions alternatively around the origin. Namely, QWRWs are highly likely locked in around the origin, which is a manifestation of localization (Fig. 3(c)). In Fig. 4(d), on the positive side (more precisely for $x \geq 10$), the relation of $p_n(x)$ and $q_n(x)$ seems to be almost the same as Ex. 1 (Fig. 4(a)). However, around the defect position

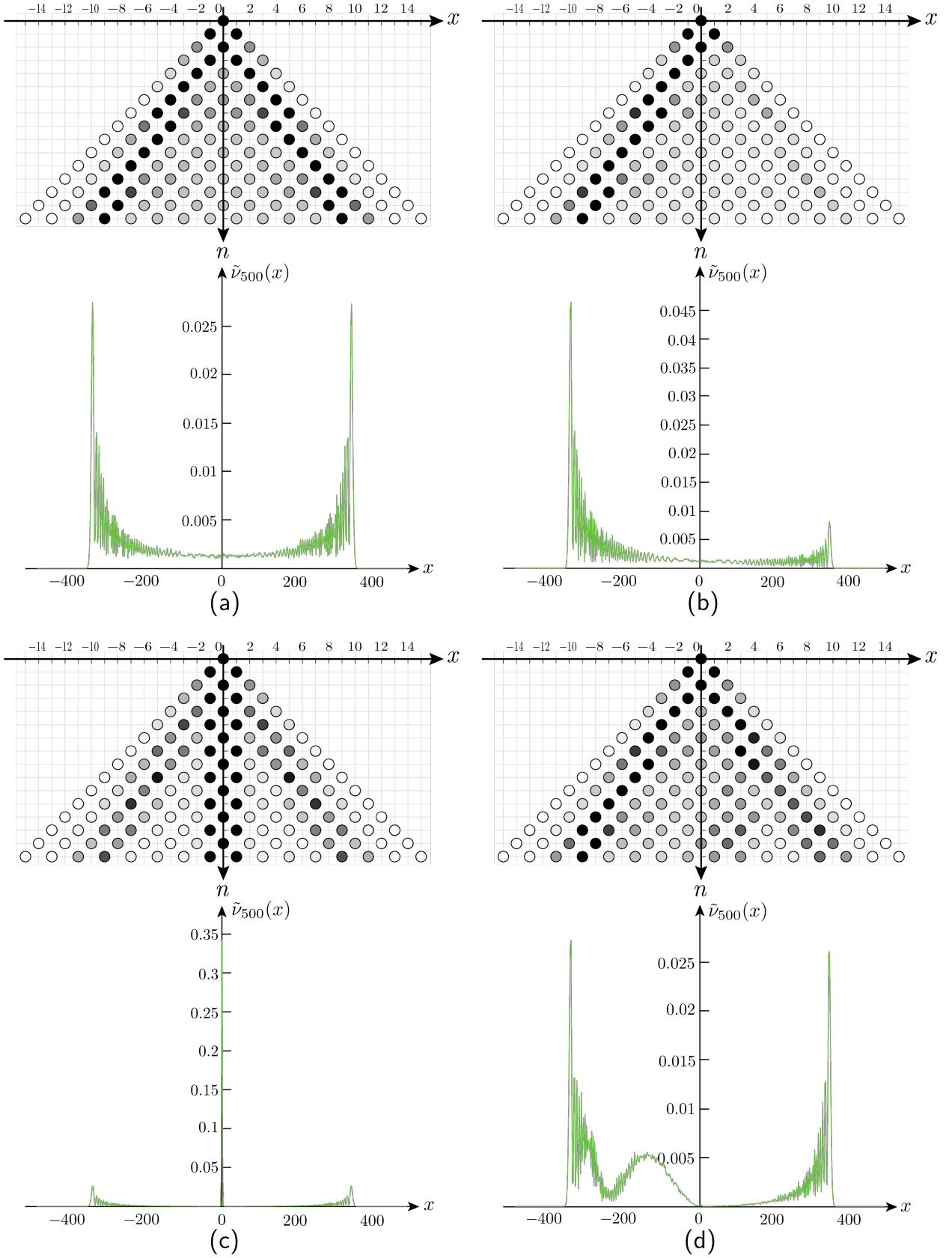


Figure 3: Graphical expressions of QWRW. The upper figure of each panel illustrates the space-time diagrams of the probability distribution. Circular markers are located at the coordinates (n, x) such that $\tilde{v}_n(x) > 0$ with their color indicating the value of $\tilde{v}_n(x)$. The darker the color is, the larger the value of $\tilde{v}_n(x)$ is. The lower figure of each panel shows probability distribution of QWRW $\tilde{v}_n(x)$ at the time instant $n = 500$, which exactly matching the distribution of the original QWs shown in Fig. 1.

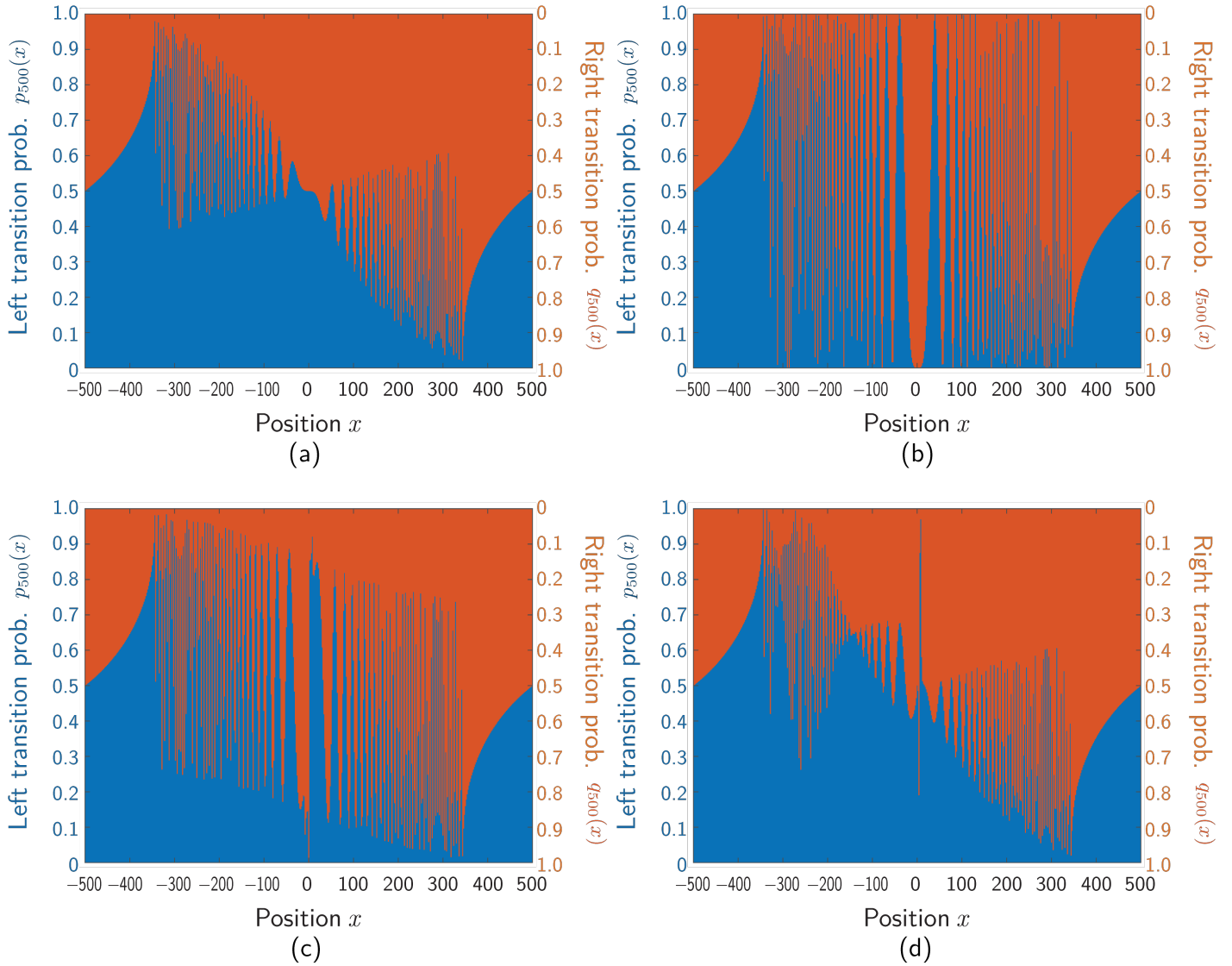


Figure 4: The transition probabilities $p_{500}(x)$ and $q_{500}(x)$ for QWRWs generated from QWs for (a) the symmetric example 1, (b) asymmetric example 2, (c) defect coin at the origin example 3, and (d) defect coin at $x = 5$ example 4. It holds that $p(x) + q(x) = 1$, so left ($p_{500}(x)$, blue) and right ($q_{500}(x)$, orange) transition probabilities are expressed as a stacked bar graph.

($x = 5$), there is a prominently high peak of $p_n(x)$ (with fluctuations) which is not observed in Ex. 1. This is considered to be a result of the defect located near the origin.

4 Individual paths and analysis of a walker's future direction

One of the significant benefits of QWRWs is that the notion of the path of a walker is valid because the walker follows a classical probability at each position. A real quantum walk is not a stochastic process, so it is not permitted to observe its path in such a classical way. In this regard, QWRW plays an important role as the visualizer of quantum walks. Here we demonstrate the path trajectories of the walkers of QWRWs.

The curves in Figs. 5(a), (b), (c), and (d) show the path trajectories of the walkers of QWRWs, which correspond to Exs. 1, 2, 3, and 4, respectively. The horizontal and vertical axis respectively

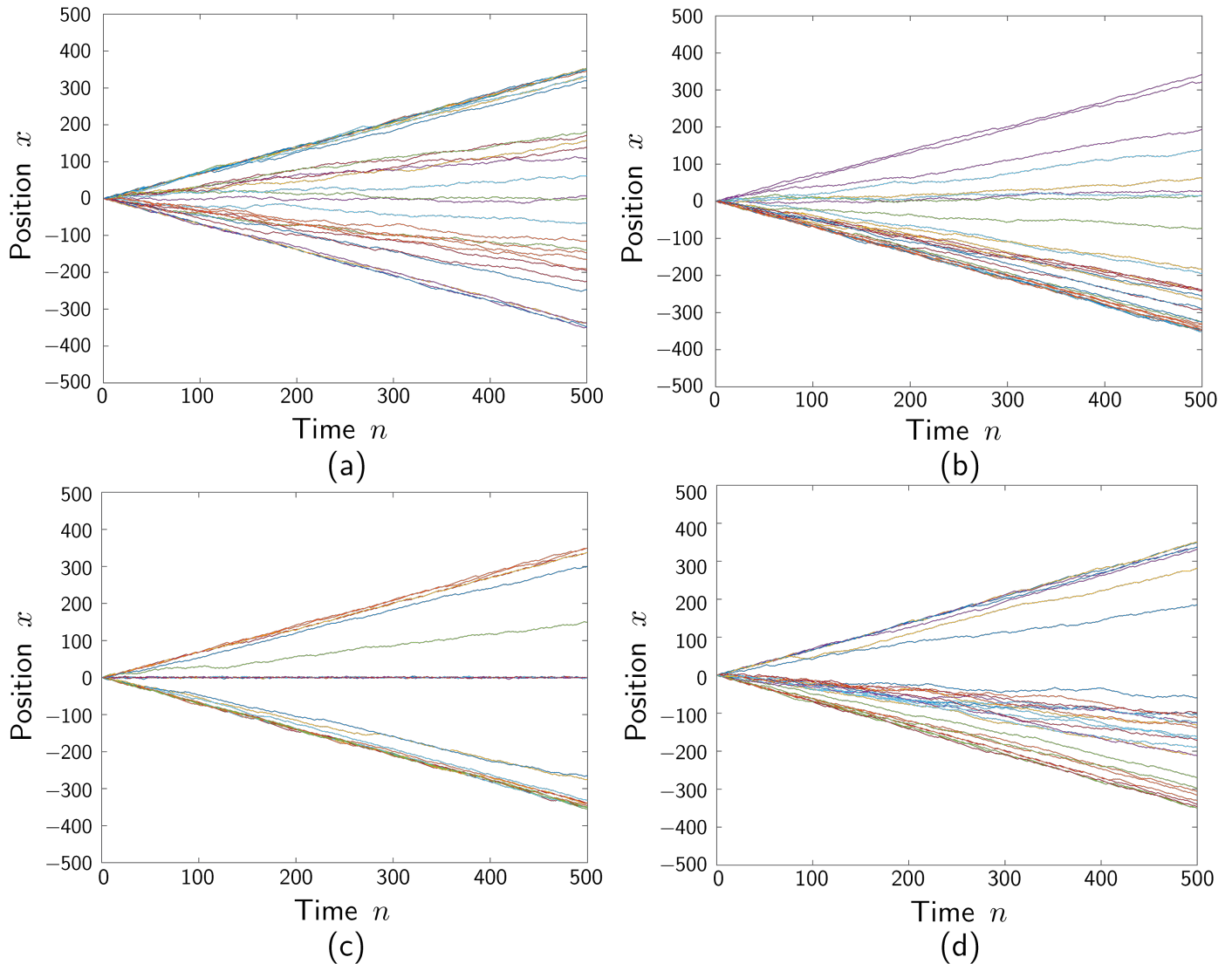


Figure 5: The paths of individual walkers in QWRWs for final time $N = 500$ and 30 walkers for (a) example 1 (symmetric case), (b) example 2 (asymmetric case), (c) example 3 (defect at origin), and (d) example 4 (defect at $x = 5$). The linear spreading of quantum walks is visible as quasi-ballistic trajectories towards the edges. Paths staying around the origin in Ex. 3 (c) localization by the defect coin in the quantum walk.

denote time and position. The number of walkers shown therein is 30. There are many paths that spread towards the end sections resulting in linear spreading. While in a true QW linear spreading is an effect of many interfering wave amplitudes, in QWRWs this effect can be observed even on the scale of an individual walker.

On the other hand, in Fig. 5(c), many walkers are wandering around the origin $x = 0$. Furthermore, in Fig. 5(d), a majority of walkers avoid going in the positive direction and choose the negative transition. Both of these trends allow the QWRWs to emulate the effects of the defect coins.

Finally, we further examine the properties made observable by QWRWs through the analysis of individual trajectories. Here, the final time instant is given by $N \in \mathbb{N}$. Let K be the number of walkers of QWRWs or the simple random walk and $S_n^{(k)}$ as the position of the k -th walkers at time n with $k \in [K]$ and $n \in [N]_0$. Moreover, using them, we define $r(n)$ as the following to characterize the relevance of the

current (time: n) position and the future (time: N) position:

$$r(n) = \frac{1}{K} \times \#\{k \in [K] \mid \text{sgn}(S_N^{(k)})\text{sgn}(S_n^{(k)}) = 1\}. \quad (65)$$

Here $\text{sgn}(S_N^{(k)})\text{sgn}(S_n^{(k)}) = 1$ means that the k -th walker is on the same side as the final position with respect to the origin at time n . On the other hand, $\text{sgn}(S_N^{(k)})\text{sgn}(S_n^{(k)}) = -1$ means that the k -th walker is on the opposite side to the final position with respect to the origin at time n . In this way, $\text{sgn}(S_N^{(k)})\text{sgn}(S_n^{(k)})$ is the benchmark to investigate when walkers effectively determine the directions they arrive in the future. If a walker maintains $\text{sgn}(S_N^{(k)})\text{sgn}(S_n^{(k)}) = 1$, we can interpret it that the walker determines their own evolving direction. Based on that, we can consider that $r(n)$ is a figure-of-merit to investigate the ratio of walkers that determines their future direction.

The red, yellow, purple, and light green curves in Fig. 6(a) show $r(n)$ regarding QWRWs of Exs. 1, 2, 3, and 4 discussed in Sect. 3, respectively. In addition, the blue curve in Fig. 6(a) indicates $r(n)$ for the simple random walk in the case of $p = q = 1/2$. We can clearly observe that $r(n)$ of QWRWs increases dramatically soon after the time evolution begins after $n = 0$, i.e. the future direction of a walker is highly determined by the initial position. This is affected by linear spreading, one of the characteristics of quantum walks.

In further consideration, the jump-up of $r(n)$ of the one-defect QWRW (Ex. 3: purple curve) is not higher than that of the no-defect QWRWs (Ex. 1: red curve and Ex. 2: yellow curve) and maintains the value within a certain range. Moreover, $r(n)$ of Ex. 4 (light green curve) shows double-jump and reaches the value 1 the fastest after the second jump. The two unique behavior should be examined in another way, so we quantitatively analyze the variance of $r(n)$ by the following method. We derive the 2-term moving variance (MV) $v(n)$ of $r(n)$ by the following. See Appendix A for details.

$$v(n) = \frac{1}{4}(r(n)^2 - 2r(n)r(n-1) + 5r(n-1)^2). \quad (66)$$

The results are shown in Fig. 6(b). We observe that $v(n)$ decreases dramatically right after the jump-up in QWRWs of Exs. 1, 2, and 4. Conversely, in the simple random walk and QWRW of Ex. 3, $v(n)$ does not exhibit a drastic decrease, which stays at a constant value of approximately 10^{-2} . This means that many walkers of the one-defect QWRW wander around the origin right before the final time; that is the effect of the other characteristics of quantum walks: localization. On the other hand, in QWRW of Ex. 4, $v(n)$ becomes the smallest of the five samples and at several time instants reaches 0. This indicates that all walkers leave the origin and go in the determined direction in a certain amount of time. This is considered to be the escape from the defect point near (but not on) the origin; which is another effect of localization.

5 Summary and discussion

In summary, we mathematically formulated a discrete one-dimensional quantum-walk-replicating random walk (QWRW) and proved that its resultant probability distribution is identical to the original quantum walk (QW). Furthermore, we analyzed the behavior of the walkers of QWRWs by examining the time- and position-dependent probability as well as transition probability toward the left and right sides. We can clearly observe linear spreading and localizations in the graphical representations of QWRW, which are completely inherited from the original quantum walk. We can also observe intricate patterns for the transition probabilities of QWRWs, resulting from the strong self-interference of the original QWs.

Moreover, we demonstrated that QWRWs determine their future traveling directions shortly after their departure from the origin, which is contrasting characters compared with classical random walks.

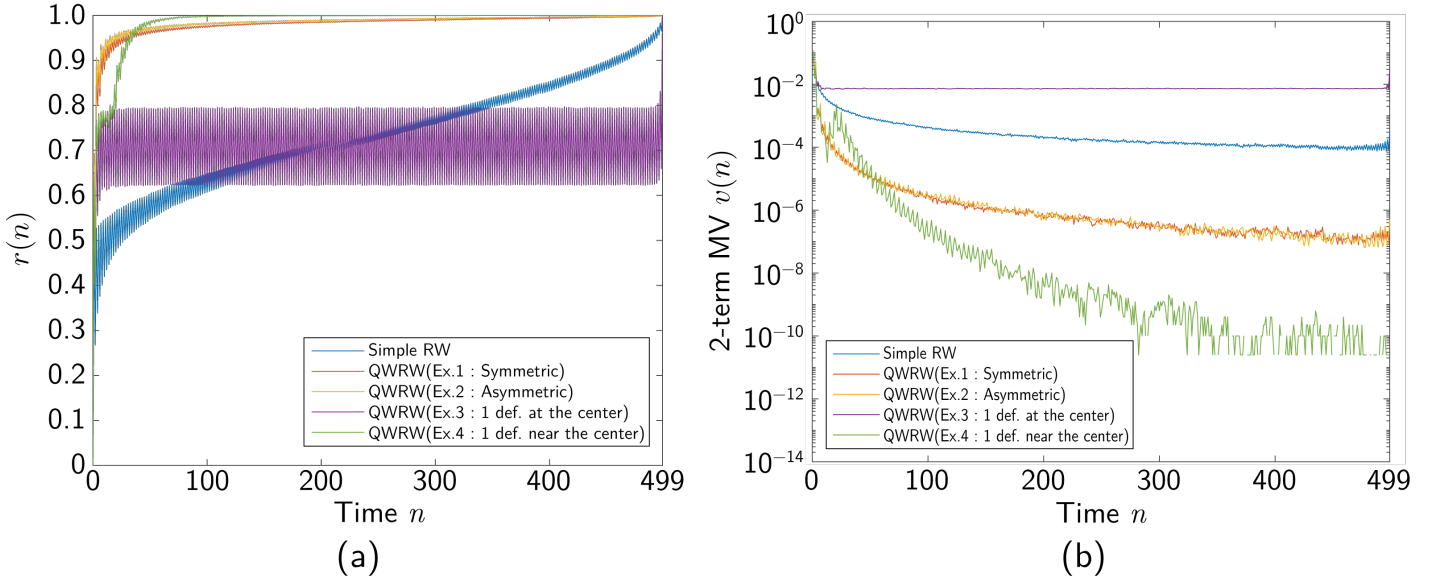


Figure 6: (a) The degree of deciding future direction is characterized through the analysis of paths derived via QWRWs or the simple random walk ($N = 499$, $K = 100000$). QWRWs of Exs. 1 and 2 exhibit a dramatic increase right after the initial time, which is another manifestation of linear spreading. (b) The 2-term moving variance (MV) $v(n)$ of $r(n)$. QWRW of Ex. 3 exhibits a larger variance, which clearly indicates localization. In QWRW of Ex. 4, $v(n)$ becomes zero at certain time n , which is excluded from the plot therein.

In this way, the QWRW model reveals the properties of quantum walks in a novel manner. This study provides new insight into quantum walks as well as its intuitive understanding, which may trigger novel applications.

For future studies, more avenues of research remain. A deeper mathematical understanding of QWRWs is desirable and several open questions remain. For example: What are the asymptotic behavior of transition probabilities $\lim_{n \rightarrow \infty} p_n(x)$ and $\lim_{n \rightarrow \infty} q_n(x)$ for each $x \in \mathbb{Z}$? Can the metrics describing the determining of future directions be represented by an analytical formula? Another interest regards explorations toward applications. Indeed, QW is considered one of the most important models to implement quantum search algorithms. Besides, Naruse et al. reported acceleration of reinforcement learning using random walks driven by chaotic dynamics [31]. This implies that a QW may be an interesting resource for solving machine learning problems. Concerning the fact that QWRW provides a classical equivalence of QW, applications studies in this direction seem promising.

Appendix A The 2-term moving variance of $r(n)$

We define 2-term moving variance $v(n)$ of $r(n)$, which we introduced in Sect. 4, along 2-term moving average $m(n)$ of $r(n)$ defined as follow. For $n \in \mathbb{N}$,

$$m(n) = \frac{1}{2}(r(n) + r(n-1)). \quad (67)$$

Here we consider $v(n)$ as the analog of the ordinary variance: the mean of the difference between the random variable and its mean. Concretely, we define

$$v(n) = \frac{1}{2}\{(r(n) - m(n))^2 + (r(n-1) - m(n))^2\}. \quad (68)$$

By substituting (67) to it, we obtain

$$v(n) = \frac{1}{4}(r(n)^2 - 2r(n)r(n-1) + 5r(n-1)^2). \quad (69)$$

Acknowledgement

This work was supported by JST SPRING, Grant Number JPMJSP2108.

References

- [1] N. Konno: Quantum Walks, In: Franz, U., Schürmann, M., (eds.) Quantum Potential Theory, Lecture Notes in Mathematics, vol. 1954, pp. 309-452. Springer, Heidelberg (2008).
- [2] J. Kempe: Quantum random walks - an introductory overview, *Contemp. Phys.*, **44**, 307-327, (2003).
- [3] S. E. Venegas-Andraca: Quantum walks: a comprehensive review, *Quantum Inf. Process.*, **11**, 1015-1106, (2012).
- [4] Y. Aharonov, L. Davidovich, and N. Zagury: Quantum random walks, *Phys. Rev. A*, **48**, 1687, (1993).
- [5] A. Ambainis, E. Bach, A. Nayak, A. Vishwanath, and J. Watrous: One-dimensional quantum walks, *Proc. of the 33rd Annual ACM Symposium on Theory of Computing*, 37-49 (2001).
- [6] N. Konno: Quantum random walks in one dimension, *Quantum Inf. Process.*, **1**, 345-354 (2002).
- [7] N. Konno: A new type of limit theorems for the one-dimensional quantum random walk, *J. Math. Soc. Japan*, **57**, 4 (2005).
- [8] N. Inui, N. Konno, and E. Segawa: One-dimensional three-state quantum walk, *Phys. Rev. E*, **72**, 056112 (2005).
- [9] K. Watabe, N. Kobayashi, M. Katori and N. Konno: Limit distributions of two-dimensional quantum walks, *Phys. Rev. A*, **77**, 062331 (2008).
- [10] N. Konno: Localization of an inhomogeneous discrete-time quantum walk on the line, *Quantum Inf. Process.*, **9** 405-418 (2010).
- [11] T. Sunada and T. Tate: Asymptotic behavior of quantum walks on the line, *J. Funct. Anal.*, **262** (6), 2608-2645 (2012).
- [12] N. Konno, T. Łukzak, and E. Segawa: Limit measures of inhomogeneous discrete-time quantum walks in one dimension, *Quantum Inf. Process.*, **12**, 33-53 (2013).
- [13] T. Machida: A localized quantum walk with a gap in distribution, *Quantum Inf. Comput.*, **16** (5&6), 515-529 (2016).
- [14] T. Yamagami, E. Segawa, and N. Konno: General condition of quantum teleportation by one-dimensional quantum walks, *Quantum Inf. Process.*, **20**, 224 (2021).
- [15] Y. Wang, Y. Shang, and P. Xue: Generalized teleportation by quantum walks, *Quantum Inf. Process.*, **16**, 221 (2017).

- [16] N. Konno: A new time-series model based on quantum walk, *Quantum Stud.: Math. Found.*, **6**, 61-72 (2019).
- [17] J. K. Asbóth and H. Obuse: Bulk-boundary correspondence for chiral symmetric quantum walks, *Phys. Rev. B*, **88**, 121406(R) (2013).
- [18] H. Obuse, J. K. Asbóth, Y. Nishimura, and N. Kawakami: Unveiling hidden topological phases of a one-dimensional Hadamard quantum walk, *Phys. Rev. B*, **92**, 045424 (2015).
- [19] L. Matsuoka, A. Ichihara, M. Hashimoto, and K. Yokoyama: Theoretical study for laser isotope separation of heavy-element molecules in a thermal distribution, *International Conference on Toward and Over the Fukushima Daiichi Accident (GLOBAL 2011)*, Chiba (2011).
- [20] A. Ichihara, L. Matsuoka, E. Segawa, and K. Yokoyama: Isotope-selective dissociation of diatomic molecules by terahertz optical pulses, *Phys. Rev. A*, **91**, 043404 (2015).
- [21] Y. Ide, N. Konno, S. Matsutani, and H. Mitsuhashi: New theory of diffusive and coherent nature of optical wave via a quantum walk, *Annals of Physics*, **383**, 164-180 (2017).
- [22] E. Renshaw and R. Henderson: The correlated random walk, *J. Appl. Prob.*, **18**, 403-414 (1981).
- [23] V. Zaburdaev, S. Denisov, and J. Klafter: Lévy walks, *Rev. Mod. Phys.*, **87**, 483 (2015).
- [24] Y. Nonaka, H. Ono, K. Sadakane, and M. Yamashita: The hitting and cover times of Metropolis walks, *Theor. Comput. Sci.*, **411** (16-18), 1889-1894 (2010).
- [25] M. S. Abe: Functional advantages of Lévy walks emerging near a critical point, *PNAS*, **117** (39), 24336-24344 (2020).
- [26] E. Scalas: The application of continuous-time random walks in finance and economics, *Physica A*, **362** (2), 225-239 (2006).
- [27] F. Fouss, A. Pirotte, J.-M. Renders, and M. Saerens: Random-walk computation of similarities between nodes of a graph with application to collaborative recommendation, *IEEE Transactions on Knowledge and Data Engineering*, **19** (3), 355-369 (2007).
- [28] M. G. Andrade, F. de Lima Marquezino, and D. R. Figueiredo: On the equivalence between quantum and random walks on finite graphs, *Quantum Inf. Process.*, **19**, 417 (2020).
- [29] A. Romanelli, A. C. Sicardi Schifino, R. Siri, G. Abal, A. Auyuanet, and R. Donangelo: Quantum random walk on the line as a Markovian process, *Physica A*, **338**, 395-405 (2004).
- [30] M. Montero: Quantum and random walks as universal generators of probability distributions, *Phys. Rev. A*, **95**, 062326 (2017).
- [31] M. Naruse, T. Mihara, H. Hori, H. Saigo, K. Okamura, M. Hasegawa, and A. Uchida: Scalable photonic reinforcement learning by time-division multiplexing of laser chaos, *Sci. Rep.*, **8**, 10890 (2018).